Scaling TransNormer to 175 Billion Parameters

[2]**Zhen Qin**[♯], [1,2]**Dong Li**[♯], [1,2]**Weigao Sun**[♯], [1,2]**Weixuan Sun**[♯], [1,2]**Xuyang Shen**[♯],
[2]**Xiaodong Han**, [2]**Yunshen Wei**, [2]**Baohong Lv**, [1]**Fei Yuan**, [2]**Xiao Luo**,
[1]**Yu Qiao**, [1,2]**Yiran Zhong**[*]
[1]Shanghai AI Laboratory, [2]OpenNLPLab
https://github.com/OpenNLPLab/TransnormerLLM

Abstract

We present TransNormerLLM, the first linear attention-based Large Language Model (LLM) that outperforms conventional softmax attention-based models in terms of both accuracy and efficiency. TransNormerLLM evolves from the previous linear attention architecture TransNormer [32] by making advanced modifications that include positional embedding, linear attention acceleration, gating mechanism, tensor normalization, and inference acceleration and stabilization. Specifically, we use LRPE [34] together with an exponential decay to avoid attention dilution issues while allowing the model to retain global interactions between tokens. Additionally, we propose Lightning Attention, a cutting-edge technique that accelerates linear attention by more than twice in runtime and reduces memory usage by a remarkable four times. To further enhance the performance of TransNormer, we leverage a gating mechanism to smooth training and a new tensor normalization scheme to accelerate the model, resulting in an impressive acceleration of over 20%. Furthermore, we have developed a robust inference algorithm that ensures numerical stability and consistent inference speed, regardless of the sequence length, showcasing superior efficiency during both training and inference stages. Scalability is at the heart of our model's design, enabling seamless deployment on large-scale clusters and facilitating expansion to even more extensive models, all while maintaining outstanding performance metrics. Rigorous validation of our model design is achieved through a series of comprehensive experiments on our self-collected corpus, boasting a size exceeding 6TB and containing over 2 trillion tokens. To ensure data quality and relevance, we implement a new self-cleaning strategy to filter our collected data. we plan to open-source our pre-trained models, fostering community-driven advancements in the field and positioning our work as a stepping-stone toward exploring efficient transformer structures in LLMs.

1 Introduction

The field of Natural Language Processing (NLP) has been revolutionized by the advent of large-scale language models (LLMs) [43, 2, 3]. These models have demonstrated exceptional performance across a multitude of tasks, elevating abilities to comprehend, generate, and interact with human languages in computational frameworks. Previous language modeling development has predominantly centered around Transformer architectures, with seminal models such as vanilla Transformer [44], GPT series [36, 37, 3], BERT [10], and BART [24] standing as standard backbones in related fields. The success of Transformer architectures is premised on the softmax attention mechanism, which discerns dependencies among input tokens in a data-driven scheme and has global position awareness, offering the model an effective way to handle the long-range dynamism of natural language.

---

[*]Yiran Zhong is the corresponding author. Email: zhongyiran@gmail.com. ♯ indicates equal contribution.

Table 1: **TransNormerLLM Model Variants.**

Model Size	Non-Embedding Params	Layers	Model Dim	Heads	Equivalent Models
385M	384,974,848	24	1024	8	Pythia-410M
1B	992,165,888	16	2048	16	Pythia-1B
3B	2,876,006,400	32	2560	20	Pythia-2.8B
7B	6,780,547,072	30	4096	32	LLAMA-6.7B
13B	12,620,195,840	36	5120	40	LLAMA-13B
65B	63,528,009,728	72	8192	64	LLAMA-65B
175B	173,356,498,944	88	12288	96	GPT-3

Nevertheless, conventional Transformers are not without their constraints. Primarily, their quadratic time complexity with respect to the sequence length limits their scalability and hampers efficiency in terms of computational resources and time during the training and inference stages. Numerous efficient sequence modeling methods have been proposed in an attempt to reduce the quadratic time complexity to linear [21, 5, 33, 49, 48]. However, there are two reasons that prohibit them to be applied to LLMs: 1) their performance in language modeling is often unsatisfactory; 2) they do not demonstrate speed advantages in real-world scenarios.

In this paper, we introduce TransNormerLLM, the first linear attention-based LLM that surpasses conventional softmax attention in both accuracy and efficiency. The development of TransNormer-LLM builds upon the foundations of the previous linear attention architecture, TransNormer [32], while incorporating a series of advanced modifications to achieve superior performance. The key enhancements in TransNormerLLM include positional embedding, linear attention acceleration, gating mechanism, tensor normalization, and inference acceleration.

One notable improvement is the replacement of the TransNormer's DiagAttention with Linear Attention to enhance global interactions. To address the issue of dilution, we introduced LRPE [34] with exponential decay. Lightning Attention, a novel technique that significantly accelerates linear attention during training is introduced, resulting in a more than two-fold improvement, while also reducing memory usage by four times with IO awareness. Furthermore, we simplified GLU and Normalization, with the latter leading to a 20% overall speedup. A robust inference algorithm ensures the stability of numerical values and constant inference speed, regardless of the sequence length, thereby enhancing the efficiency of our model during both training and inference stages.

To validate the efficacy of TransNormerLLM, we meticulously collect a large corpus that is more than 6TB in size and contains over 2 trillion tokens. We develop a new self-cleaning strategy to filter the collected corpus to ensure data quality. We expand the original TransNormer model ranging from 385M to 175B parameters as illustrated in Table 1 and conduct a series of comprehensive experiments and ablations on our corpus, demonstrating superior performance to softmax attention-based methods as well as faster training and inference speed.

We are committed to fostering community-driven advancements in the field of LLMs. To this end, we plan to open-source our pre-trained models, enabling researchers and practitioners to build upon our work and explore efficient transformer structures in LLMs.

2 Related Work

2.1 Transformer-based LLMs

In recent years, the field of Large Language Models (LLMs) has experienced significant advancements. Adhering to the scaling laws [20], various LLMs with over 100 billion parameters have been introduced, such as GPT-3 [3], Gopher [38], PaLM [6], GLM [11] and *etc.*. More specialized models like Galactica [41] have also emerged for specific domains like science. A notable development is Chinchilla [17], an LLM model with 70 billion parameters that redefines these scaling laws, focusing on the number of tokens rather than model weights. Furthermore, LLaMA [43] has also sparked interest due to its promising performance and open-source availability. The discourse around LLMs also encompasses the dynamics between open-source and closed-source models. Open-source models such as BLOOM [45], OPT [46], LLaMA [43], Pythia [2] and Falcon [28] are rising to compete against their closed-source counterparts, including GPT-3 [3] and Chinchilla [17]. To speed up

training, Sparse Attention [4, 1] was introduced, but among large models, only GPT-3 adopted it [3, 39].

2.2 Non-Transformer-based LLMs Candidates

Despite the proliferation of Transformer-based large models in the research community, a portion of recent work has prioritized addressing its square space-time complexity. This focus has led to the exploration and development of a series of model architectures that diverge from the traditional Transformer structure. Among them, four significant contenders—linear transformers, state space model, long convolution, and linear recurrence—have shown promising results as substitutes for self-attention (SA) modules when modeling long sequences. These alternatives are favored for their superior asymptotic time complexity and competitive performances.

Linear Transformer   Linear Transformer decomposes Softmax Attention into the form of the inner product of hidden representations, which allows it to use the "Right Product Trick," where the product of keys and values is computed to avoid the quadratic $n \times n$ matrix. Different methods utilize various hidden representations. For example, [21] uses 1+elu as an activation function, [33] uses the cos function to approximate the properties of softmax, and [22, 48, 49] approximates softmax through theoretical approaches. Although its theoretical complexity is $O(nd^2)$, the actual computational efficiency of Linear Attention becomes quite low when used in causal attention due to the need for *cumsum* operations [18]. On the other hand, most Linear Transformers still exhibit a certain performance gap compared to traditional Transformers [21, 25].

State Space Model   State Space Model is based on the State Space Equation for sequence modeling [15], using special initialization [13, 14], diagonalization assumptions [16], and some techniques [9] to achieve performance comparable to Transformers. On the other hand, due to the characteristics of the State Space Equation, it enables inference to be conducted within constant complexity [15].

Long Convolution   Long convolution models [31, 12] utilize a kernel size equal to the input sequence length, facilitating a wider context compared to traditional convolutions. Training these models involves the efficient $O(n \log n)$ Fast Fourier Transforms (FFT) algorithm. However, long convolutions pose certain challenges, such as the need for causal convolution inference, which necessitates caching all historical computations similar to SA's key-value (KV) cache. The memory requirements for handling long sequences, coupled with the higher inference complexity compared to RNNs, make them less ideal for processing long sequences.

Linear RNN   Linear RNNs, in contrast, stand out as more suitable replacements for SA in long-sequence modeling. A notable example is the RWKV [29] model, a linear RNN-based LLM that has shown competitive performance against similarly scaled GPT models.

3   TransNormerLLM

3.1   Architecture Improvement

In this section, we thoroughly investigate each module of the network and propose several improvements to achieve an optimal balance between efficiency and performance. Below, we outline the key designs of each block along with the inspiration behind each change. We conduct an ablation study on each of these modifications in Sec. 5.

3.1.1   Improvement 1: Position encoding

In TransNormer, DiagAttention is used at the lower layers to avoid dilution issues. However, this leads to a lack of global interaction between tokens. In TransNormerLLM, we leverage LRPE [34] with exponential decay [30, 31] to address this issue, retaining full attention at the lower layers. The overall expression of our position encoding is as follows:

$$a_{st} = \mathbf{q}_s^\top \mathbf{k}_t \lambda^{s-t} \exp^{i\theta(s-t)} . \tag{1}$$

which we call it LRPE-d - Linearized Relative Positional Encoding with exponential decay. Similar to the original LRPE, we set θ to be learnable.

Note that this position encoding is fully compatible with Linear Attention, as it can be decomposed with respect to s and t separately. The value of λ for the h-th head in the l-th layer (assuming there are a total of H heads and L layers) is given by:

$$\lambda = \exp\left(-\frac{8h}{H} \times \left(1 - \frac{l}{L}\right)\right). \tag{2}$$

Here, $\frac{8h}{H}$ corresponds to the decay rate of the h-th head, while $\left(1 - \frac{l}{L}\right)$ corresponds to the decay rate of the l-th layer. The term $\left(1 - \frac{l}{L}\right)$ ensures that the Theoretical Receptive Fields (TRF) [35] at the lower layers is smaller compared to the higher layers, which aligns with TransNormer's motivation. It should be noted that the decay rate in the last layer is set to 1, allowing each token to attend to global information. We choose λ to be non-learnable since we empirically found that gradients become unstable when λ is learnable, leading to NaN values.

3.1.2 Improvement 2: Gating mechanism

Gate can enhance the performance of the model and smooth the training process. In TransNormer-LLM, we adopted the approach from Flash [18] and used the structure of Gated Linear Attention (GLA) in token mixing:

$$\text{TokenMixer} : \mathbf{O} = \text{Norm}(\mathbf{Q}\mathbf{K}^\top\mathbf{V}) \odot \mathbf{U}, \tag{3}$$

where:

$$\mathbf{Q} = \phi(\mathbf{X}\mathbf{W}_q), \mathbf{K} = \phi(\mathbf{X}\mathbf{W}_k), \mathbf{V} = \mathbf{X}\mathbf{W}_v, \mathbf{U} = \mathbf{X}\mathbf{W}_u. \tag{4}$$

We chose ϕ to be $1 + elu$. We found that the specific choice of ϕ has a minimal impact on the results, as shown in Table 8.

To further accelerate the model, we propose Simple GLU (SGLU), which removes the activation function from the original GLU structure as the gate itself can introduce non-linearity. Therefore, our channel mixing becomes:

$$\text{ChannelMixer} : \mathbf{O} = [\mathbf{V} \odot \mathbf{U}]\mathbf{W}_o, \mathbf{V} = \mathbf{X}\mathbf{W}_v, \mathbf{U} = \mathbf{X}\mathbf{W}_u, \tag{5}$$

We empirically find that not using an activation function does not lead to any performance loss, as demonstrated in Table 9.

3.1.3 Improvement 3: Tensor normalization

We employ the NormAttention introduced in TransNormer [32] as follows:

$$\mathbf{O} = \text{Norm}((\mathbf{Q}\mathbf{K}^\top)\mathbf{V}) \tag{6}$$

This attention mechanism eliminates the softmax and scaling operation. Moreover, it can be transformed into linear attention through right multiplication:

$$\mathbf{O} = \text{Norm}(\mathbf{Q}(\mathbf{K}^\top\mathbf{V})) \tag{7}$$

This linear form allows for recurrent prediction with a complexity of $O(nd^2)$, making it efficient during inference. Specifically, we only update $\mathbf{K}^\top\mathbf{V}$ in a recurrent manner without computing the full attention matrix. In TransNormerLLM, we replace the RMSNorm with a new simple normalization function called SimpleRMSNorm, abbreviated as SRMSNorm:

$$\text{SRMSNorm}(\mathbf{x}) = \frac{\mathbf{x}}{\|\mathbf{x}\|_2/\sqrt{d}}. \tag{8}$$

We empirically find that using SRMSNorm does not lead to any performance loss, as demonstrated in the ablation study in Table. 10.

3.1.4 The overall structure

The overall structure is illustrated in Figure 1. In this structure, the input $\mathbf{X}$ is updated through two consecutive steps: First, it undergoes Gated Linear Attention (GLA) with the application of SimpleRMSNorm (SRMSNorm) normalization. Then, it goes through the Simple Gated Linear Unit (SGLU) with SRMSNorm normalization again. This overall architecture helps improve the model's performance based on the PreNorm approach. The pseudo-code of the overall process is as follows:

$$\begin{aligned}\mathbf{X} &= \mathbf{X} + \text{GLA}(\text{SRMSNorm}(\mathbf{X})), \\ \mathbf{X} &= \mathbf{X} + \text{SGLU}(\text{SRMSNorm}(\mathbf{X})).\end{aligned} \quad (9)$$

3.2 Training Optimization

3.2.1 Lightning Attention

The structure of linear attention allows for efficient attention calculation with a complexity of $O(nd^2)$ through right-multiplication. However, for causal prediction, right-multiplication is not efficient as it necessitates *cumsum* computation [18], which hinders parallelism training.
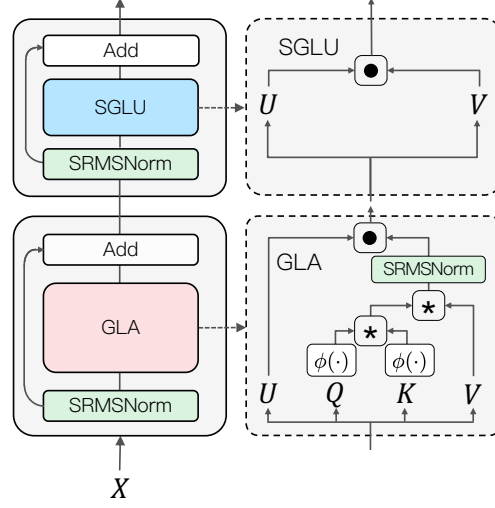

Figure 1: Architecture overview of the proposed model. Each transformer block is composed of a Simple Gated Linear Unit (SGLU) for channel mixing and a Gated Linear Attention for token mixing. We apply pre-norm for both modules.

As a result, during training, we continue to use the conventional left-multiplication version. To accelerate attention calculations, we introduce the Lightning Attention algorithm inspired by [7, 8], which makes our linear attention IO-friendly. It computes the following expression:

$$\mathbf{O} = (\mathbf{Q}\mathbf{K}^{\top} \odot \mathbf{M})\mathbf{V}. \quad (10)$$

Here, $\mathbf{M}$ is the attention mask which enables lower triangular causal masking and positional encoding. In the Lightning Attention, we split the inputs $\mathbf{Q}, \mathbf{K}, \mathbf{V}$ into blocks, load them from slow HBM to fast SRAM, then compute the attention output with respect to those blocks. Then we accumulate the final results. The computation speed is accelerated by avoiding the operations on slow HBM. The implementation details of Lightning Attention are shown in Algorithm 1 for forward pass and Algorithm 2 for backward pass. Note that there is a faster implementation for gradient computation that will be released in the future.

Algorithm 1 Lightning Attention Forward Pass

Input: $\mathbf{Q}, \mathbf{K}, \mathbf{V} \in \mathbb{R}^{n \times d}$, attention mask $\mathbf{M} \in \mathbb{R}^{n \times n}$, block sizes B_c, B_r;
Initialize: $\mathbf{O} = \mathbf{0} \in \mathbb{R}^{n \times d}$;
Divide $\mathbf{Q}$ into $T_r = \frac{n}{B_r}$ blocks $\mathbf{Q}_1, \mathbf{Q}_2, ...\mathbf{Q}_{T_r}$ of size $B_r \times d$ each.
Divide $\mathbf{K}, \mathbf{V}$ into $T_c = \frac{n}{B_c}$ blocks $\mathbf{K}_1, \mathbf{K}_2, ...\mathbf{K}_{T_c}, \mathbf{V}_1, \mathbf{V}_2, ...\mathbf{V}_{T_c}$ of size $B_c \times d$ each.
Divide $\mathbf{O}$ into $T_r = \frac{n}{B_r}$ blocks $\mathbf{O}_1, \mathbf{O}_2, ...\mathbf{O}_{T_r}$ of size $B_r \times d$ each.
Divide $\mathbf{M}$ into $T_r \times T_c$ blocks $\mathbf{M}_{11}, \mathbf{M}_{12}, ...\mathbf{M}_{T_r,T_c}$ of size $B_r \times B_c$ each.
for $1 \leq i \leq T_r$ **do**
    Load $\mathbf{Q}_i \in \mathbb{R}^{B_r \times d}$ from HBM to on-chip SRAM.
    Initialize $\mathbf{O}_i = \mathbf{0} \in \mathbb{R}^{B_r \times d}$ on SRAM.
    for $1 \leq j \leq T_c$ **do**
        Load $\mathbf{K}_j, \mathbf{V}_j \in \mathbb{R}^{B_c \times d}$ from HBM to on-chip SRAM.
        Load $\mathbf{M}_{ij} \in \mathbb{R}^{B_c \times B_c}$ from HBM to on-chip SRAM.
        On chip, compute $\mathbf{A}_{ij} = [\mathbf{Q}_i\mathbf{K}_j^{\top}] \odot \mathbf{M}_{ij} \in \mathbb{R}^{B_r \times B_c}$.
        On chip, compute $\mathbf{O}_i = \mathbf{O}_i + \mathbf{A}_{ij}\mathbf{V}_j \in \mathbb{R}^{B_r \times d}$.
    end for
    Write $\mathbf{O}_i$ to HBM as the i-th block of $\mathbf{O}$.
end for
return $\mathbf{O}$

Algorithm 2 Lightning Attention Backward Pass

Input: $\mathbf{Q}, \mathbf{K}, \mathbf{V}, \mathbf{dO} \in \mathbb{R}^{n \times d}$, attention mask $\mathbf{M} \in \mathbb{R}^{n \times n}$, on-chip SRAM of size M, block sizes B_c, B_r;
Initialize: $\mathbf{dQ} = \mathbf{dK} = \mathbf{dV} = 0 \in \mathbb{R}^{n \times d}$;
Divide $\mathbf{Q}$ into $T_r = \frac{n}{B_r}$ blocks $\mathbf{Q}_1, \mathbf{Q}_2, ... \mathbf{Q}_{T_r}$ of size $B_r \times d$ each.
Divide $\mathbf{K}, \mathbf{V}$ into $T_c = \frac{n}{B_c}$ blocks $\mathbf{K}_1, \mathbf{K}_2, ... \mathbf{K}_{T_c}, \mathbf{V}_1, \mathbf{V}_2, ... \mathbf{V}_{T_c}$ of size $B_c \times d$ each.
Divide $\mathbf{O}, \mathbf{dO}$ into $T_r = \frac{n}{B_r}$ blocks $\mathbf{O}_1, \mathbf{O}_2, ... \mathbf{O}_{T_r}, \mathbf{dO_1}, \mathbf{dO_2}, ... \mathbf{dO_{T_r}}$ of size $B_r \times d$ each
Divide $\mathbf{M}$ into $T_r \times T_c$ blocks $\mathbf{M}_{11}, \mathbf{M}_{12}, ... \mathbf{M}_{T_r,T_c}$ of size $B_r \times B_c$ each.
for $1 \leq j \leq T_c$ **do**
    Load $\mathbf{K}_j, \mathbf{V}_j \in \mathbb{R}^{B_c \times d}$ from HBM to on-chip SRAM.
    Initialize $\mathbf{dK}_j = \mathbf{dV}_j = 0 \in \mathbb{R}^{B_c \times d}$ on SRAM.
    for $1 \leq i \leq T_r$ **do**
        Load $\mathbf{Q}_i, \mathbf{O}_i, \mathbf{dO}_i \in \mathbb{R}^{B_r \times d}$ from HBM to on-chip SRAM.
        Load $\mathbf{M}_{ij} \in \mathbb{R}^{B_c \times B_c}$ from HBM to on-chip SRAM.
        Initialize $\mathbf{dK}_j = \mathbf{dV}_j = 0 \in \mathbb{R}^{B_c \times d}$ on SRAM.
        On chip, compute $\mathbf{A}_{ij} = [\mathbf{Q}_i \mathbf{K}_j^\top] \odot \mathbf{M}_{ij} \in \mathbb{R}^{B_r \times B_c}$.
        On chip, compute $\mathbf{dV}_j = \mathbf{dV}_j + \mathbf{A}_{ij}^\top \mathbf{dO}_i \in \mathbb{R}^{B_c \times d}$.
        On chip, compute $\mathbf{dA}_{ij} = [\mathbf{dO}_i \mathbf{V}_j^\top] \odot \mathbf{M}_{ij} \in \mathbb{R}^{B_r \times B_c}$.
        On chip, compute $\mathbf{dK}_j = \mathbf{dk}_j + \mathbf{dA}_{ij}^\top \mathbf{V}_j \in \mathbb{R}^{B_c \times d}$.
        Load $\mathbf{dQ}_i$ from HBM to SRAM, then on chip, compute $\mathbf{dQ}_i = \mathbf{dK}_i + \mathbf{dA}_{ij} \mathbf{K}_j \in \mathbb{R}^{B_r \times d}$,
        write back to HBM.
    end for
    Write $\mathbf{dK}_j, \mathbf{dV}_j$ to HBM as the j-th block of $\mathbf{dK}, \mathbf{dV}$.
end for
retun $\mathbf{dQ}, \mathbf{dK}, \mathbf{dV}$

3.2.2 Model Parallelism

To effectively carry out the large-scale pre-training of TransNormerLLM, we have focused our efforts on system optimization from a variety of angles. It is critical to emphasize that the term "large-scale" refers to two aspects: first, the model has a large number of parameters, and second, the computational infrastructure has a large number of GPU nodes. These factors result in a variety of practical challenges, including GPU memory constraints, decreased computation efficiency, slow communication speeds, *etc.*. Addressing these issues is critical to the successful implementation of the large-scale pre-training process.

We use the Fully Sharded Data Parallel (FSDP) [47] approach in our study to distribute all model parameters, gradients, and optimizer state tensors across the entire cluster. This strategic partitioning reduces memory occupancy on each individual GPU, optimizing memory utilization. To improve efficiency even further, we use Activation Checkpointing [40], which reduces the number of activations cached in memory during the backward pass. Instead, when calculating the gradients, these activations are removed and recomputed. This technique aids in more efficient computations and resource conservation. Furthermore, we use Automatic Mixed Precision (AMP) [26] to reduce GPU memory consumption while also accelerating computation speed. It is worth noting that throughout our experiments, we utilize BFloat16 [19] due to its observed beneficial impact on the training stability of large TransNormerLLM models.

In addition to the aforementioned efforts, we go deeper into system engineering optimization by performing model parallelism on linear transformers, which is heavily inspired by Nvidia's Megatron-LM model parallelism [40]. Each transformer layer in the conventional transformer model consists of a self-attention block followed by a two-layer multi-layer perceptron (MLP) block. When using Megatron-LM model parallelism, it is used independently on these two blocks. Similarly, within the TransNormerLLM structure, which is also made up of two main blocks, SGLU and GLA, we perform model parallelism on each of them separately. The detailed model parallelism strategies are shown below.

Model Parallelism on SGLU Recall the SGLU structure in Eq. 5:

$$\mathbf{O} = [(\mathbf{X}\mathbf{W}_v) \odot (\mathbf{X}\mathbf{W}_u)]\mathbf{W}_o, \tag{11}$$

Algorithm 3 Origin Inference Algorithm	**Algorithm 4** Robust Inference Algorithm

Input: $\mathbf{q}_t, \mathbf{k}_t, \mathbf{v}_t, t = 1, \ldots, n$;
Output: $\mathbf{o}_t, t = 1, \ldots, n$;
Initialize: $[\mathbf{kv}]_0 = \mathbf{0}$;
for $t = 1, \ldots, n$ **do**
$\quad [\mathbf{kv}]_t = [\mathbf{kv}]_{t-1} + \mathbf{k_t}\lambda^{-t}\mathbf{v}_t^\top$,
$\quad \mathbf{o}_t = \mathbf{q}_t\lambda^t[\mathbf{kv}]_t$.
end for
	Input: $\mathbf{q}_t, \mathbf{k}_t, \mathbf{v}_t, t = 1, \ldots, n$;
	Output: $\mathbf{o}_t, t = 1, \ldots, n$;
	Initialize: $[\overline{\mathbf{kv}}]_0 = \mathbf{0}$;
	for $t = 1, \ldots, n$ **do**
	$\quad [\overline{\mathbf{kv}}]_t = \lambda[\overline{\mathbf{kv}}]_{t-1} + \mathbf{k_t}\mathbf{v}_t^\top$,
	$\quad \mathbf{o}_t = \mathbf{q}_t[\overline{\mathbf{kv}}]_t$.
	end for

Its model parallel version goes with:

$$[\mathbf{O}'_1, \mathbf{O}'_2] = \mathbf{X}[\mathbf{W}_v^1, \mathbf{W}_v^2] \odot \mathbf{X}[\mathbf{W}_u^1, \mathbf{W}_u^2], \tag{12}$$

$$= [\mathbf{X}\mathbf{W}_v^1, \mathbf{X}\mathbf{W}_v^2] \odot [\mathbf{X}\mathbf{W}_u^1, \mathbf{X}\mathbf{W}_u^2], \tag{13}$$

which split the weight matrices $\mathbf{W}_v$ and $\mathbf{W}_u$ along their column and obtain an output matrix split along its column too. Then the separated output $[\mathbf{O}_1, \mathbf{O}_2]$ is multiplied by another matrix which is split along its row as:

$$\mathbf{O} = [\mathbf{O}'_1, \mathbf{O}'_2] \begin{bmatrix} \mathbf{W}_o^1 \\ \mathbf{W}_o^2 \end{bmatrix} = \mathbf{O}'_1\mathbf{W}_o^1 + \mathbf{O}'_2\mathbf{W}_o^2 \tag{14}$$

This whole procedure splits three GEMMs into the SGLU blocks across multiple GPUs and introduces only a single all-reduce operation in both the forward and backward passes, respectively.

Model Parallelism on GLA Recall the GLA block in Eqs. 3 and 4, model parallelism on GLA as follows:

$$[\mathbf{O_1}, \mathbf{O_2}] = \mathrm{SRMSNorm}(\mathbf{Q}\mathbf{K}^\top\mathbf{V}) \odot \mathbf{U}, \tag{15}$$

where:

$$\mathbf{Q} = \phi(\mathbf{X}[\mathbf{W}_q^1, \mathbf{W}_q^2]) = [\phi(\mathbf{X}\mathbf{W}_q^1), \phi(\mathbf{X}\mathbf{W}_q^2)], \tag{16}$$

$$\mathbf{K} = \phi(\mathbf{X}[\mathbf{W}_k^1, \mathbf{W}_k^2]) = [\phi(\mathbf{X}\mathbf{W}_q^1), \phi(\mathbf{X}\mathbf{W}_q^2)], \tag{17}$$

$$\mathbf{V} = \mathbf{X}[\mathbf{W}_v^1, \mathbf{W}_v^2], \mathbf{U} = \mathbf{X}[\mathbf{W}_u^1, \mathbf{W}_u^2], \tag{18}$$

Note that in implementation, we use the combined QKVU projection to improve computation efficiency. The obtained split output matrix $[\mathbf{O_1}, \mathbf{O_2}]$ again is multiplied by a weight matrix split along its column axis which is similar to Eq. 14.

3.3   Robust Inference

In this section, we discuss the inference problem in TransNormerLLM. It is important to note that the formula 1 can be decomposed into the following form:

$$a_{st} = (\mathbf{q}_s\lambda^s \exp^{i\theta s})^\top(\mathbf{k}_t\lambda^{-t} \exp^{i\theta t}). \tag{19}$$

This allows TransNormerLLM to perform inference in the form of an RNN [21]. Details of the procedure are shown in Algorithm 3. However, it is worth noting that $\lambda < 1$, which results in:

$$\|\mathbf{q}_s\lambda^s \exp^{i\theta s}\|_2 = \|\mathbf{q}_s\|_2\lambda^s \to 0, \|\mathbf{k}_t\lambda^{-t} \exp^{i\theta t}\|_2 = \|\mathbf{k}_t\|_2\lambda^{-t} \to \infty, \tag{20}$$

leading to numerical precision issues.

To avoid these issues, we propose a Robust Inference Algorithm in 4. Since $\|\mathbf{q}_s \exp^{i\theta s}\| = \|\mathbf{q}_s\|$, $\|\mathbf{k}_t \exp^{i\theta t}\| = \|\mathbf{k}_t\|$, for simplicity, we will omit LRPE [34] in the subsequent discussions, considering only $a_{st} = \mathbf{q}_s^\top\mathbf{k}_t\lambda^{s-t}$.

We will use induction to prove:

$$[\mathbf{kv}]_t = \lambda^{-t}[\overline{\mathbf{kv}}]_t. \tag{21}$$

Thus, both the Origin Inference Algorithm and the Robust Inference Algorithm yield the same results.

Base Case ($n = 1$):

$$\begin{aligned}
[\mathbf{kv}]_1 &= ([\mathbf{kv}]_0 + \mathbf{k_1}\lambda^{-1}\mathbf{v}_1^\top) \\
&= \lambda^{-1}(\mathbf{k_1}\mathbf{v}_1^\top) \\
&= \lambda^{-1}[\overline{\mathbf{kv}}]_1.
\end{aligned} \tag{22}$$

Thus, the base case is true. Let us assume the statement holds for $n = m - 1$, i.e., $[\mathbf{kv}]_{m-1} = \lambda^{-(m-1)}[\overline{\mathbf{kv}}]_{m-1}$. Then, when $n = m$:

$$\begin{aligned}
[\mathbf{kv}]_m &= [\mathbf{kv}]_{m-1} + \mathbf{k_m}\lambda^{-m}\mathbf{v}_m^\top \\
&= \lambda^{-(m-1)}[\overline{\mathbf{kv}}]_{m-1} + \mathbf{k_m}\lambda^{-m}\mathbf{v}_m^\top \\
&= \lambda^{-m}(\lambda[\overline{\mathbf{kv}}]_{m-1} + \mathbf{k_m}\mathbf{v}_m^\top) \\
&= \lambda^{-m}[\overline{\mathbf{kv}}]_m,
\end{aligned} \tag{23}$$

the statement holds. Therefore, by induction, the statement holds for all $n \geq 1$.

4   Corpus

We gather an extensive corpus of publicly accessible text from the internet, totaling over 700TB in size. The collected data are processed by our data preprocessing procedure as shown in Figure 2, leaving a 6TB cleaned corpus with roughly 2 trillion tokens. We categorize our data sources to provide better transparency and understanding. The specifics of these categories are outlined in Table 2.
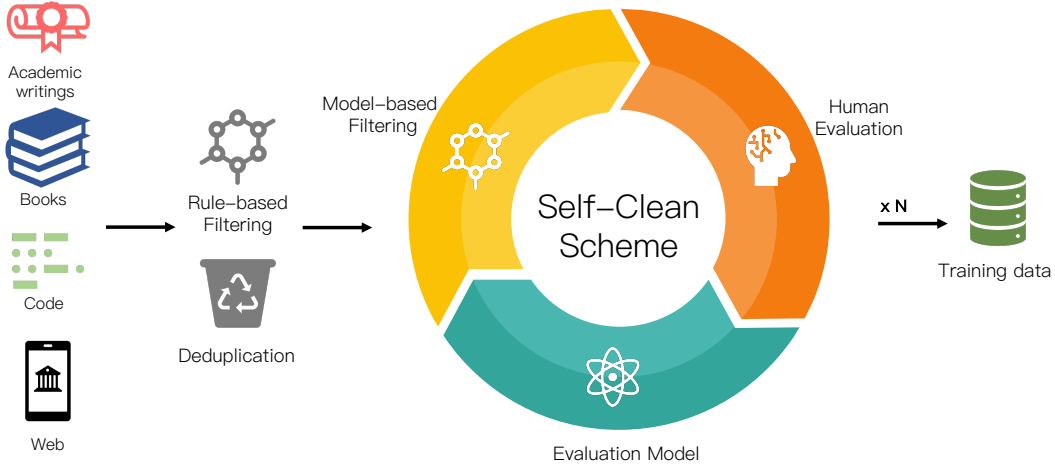
4.1   Data Preprocessing

Figure 2: **Data Preprocess Procedure.** The collected data undergoes a process of rule-based filtering and deduplication, followed by our self-clean data processing strategy: model-based filtering, human evaluation, and evaluation model. After several iterations of the above cycle, we obtain high-quality training data at around 2T tokens.

Our data preprocessing procedure consists of three steps: 1). rule-based filtering, 2). deduplication, and 3). a self-cleaning scheme. Before being added to the training corpus, the cleaned corpus needs to be evaluated by humans.

Rule-based filtering   The rules we used to filter our collected data are listed as follows:

- *Removal of HTML Tags and URLs:* The initial step in our process is the elimination of HTML tags and web URLs from the text. This is achieved through regular expression techniques that identify these patterns and remove them, ensuring the language model focuses on meaningful textual content.

Table 2: **Statistics of our corpus.** For each category, we list the number of epochs performed on the subset when training on the 2 trillion tokens, as well as the number of tokens and disk sizes. We also list the table on the right according to the language distribution.

Dataset	Epochs	Tokens	Disk size
Academic Writings	1.53	200 B	672 GB
Books	2.49	198 B	723 GB
Code	0.44	689 B	1.4 TB
Encyclopedia	1.51	5 B	18 GB
Filtered Webpages	1.00	882 B	3.1 TB
Others	0.63	52 B	154 GB
Total	-	2026 B	6 TB

Language	Tokens	Disk size
English	743 B	2.9 TB
Chiese	555 B	1.7 TB
Code	689 B	1.4 TB
Others	39 B	89 GB
Total	2026 B	6 TB

- *Elimination of Useless or Abnormal Strings:* Subsequently, the cleaned dataset undergoes a second layer of refinement where strings that do not provide value, such as aberrant strings or garbled text, are identified and excised. This process relies on predefined rules that categorize certain string patterns as non-contributing elements.
- *Deduplication of Punctuation Marks:* We address the problem of redundant punctuation marks in the data. Multiple consecutive punctuation marks can distort the natural flow and structure of sentences when training the model. We employ a rule-based system that trims these duplications down to a single instance of each punctuation mark.
- *Handling Special Characters:* Unusual or special characters that are not commonly part of the language's text corpus are identified and either removed or replaced with a standardized representation.
- *Number Standardization:* Numerical figures may be presented in various formats across different texts. These numbers are standardized into a common format to maintain consistency.
- *Preservation of Markdown/LaTeX Formats:* While removing non-textual elements, exceptions are made for texts in Markdown and LaTeX formats. Given their structured nature and ubiquitous use in academia and documentation, preserving these formats can enhance the model's ability to understand and generate similarly formatted text.

Deduplication   To ensure the uniqueness of our data and avert the risk of overfitting, we employ an efficient de-duplication strategy at the document or line level using MinHash and Locality-Sensitive Hashing (LSH) algorithms. This combination of MinHash and LSH ensures a balance between computational efficiency and accuracy in the deduplication process, providing a robust mechanism for data deduplication and text watermark removal.

Self-cleaning scheme   Our data self-cleaning process involves an iterative loop of the following three steps to continuously refine and enhance the quality of our dataset. An issue of using model-based data filters is that the filtered data will have a similar distribution as the evaluation model, which may have a significant impact on the diversity of the training data. Assuming that the majority of the pre-processed data is of high quality, we can train an evaluation model on the entire set of pre-processed data, and the model will automatically smooth the data manifold distribution and outlet low-quality data while retaining the majority of the diversities.

The self-cleaning scheme unfolds as follows:

- *Evaluation Model:* We train a 385M model on the pre-processed corpus to act as a data quality filter.
- *Model-Based Data Filtering:* We use the evaluation model to assess each piece of data with perplexity. Only data achieving a score above a certain threshold is preserved for the next step. Low-quality data are weeded out at this stage.
- *Human Evaluation:* We sample a small portion of the filtered data and manually evaluate the quality.

These steps are repeated in cycles, with each iteration improving the overall quality of the data and ensuring the resulting model is trained on relevant, high-quality text. This self-cleaning process provides a robust mechanism for maintaining data integrity, thereby enhancing the performance of the resulting language model.

4.2 Tokenization

We tokenize the data with the Byte-Pair Encoding (BPE) algorithm. Notably, to enhance compatibility with Chinese language content, a significant number of common and uncommon Chinese characters have been incorporated into our vocabulary. In cases where vocabulary items are not present in the dictionary, the words are broken down into their constituent UTF-8 characters. This strategy ensures comprehensive coverage and flexibility for diverse linguistic input during model training.

5 Experiments

We use PyTorch [27] and Trition [42] to implement TransNormerLLM in Metaseq framework [46]. Our model is trained using Adam optimizer [23], and we employ FSDP to efficiently scale our model to NVIDIA A100 80G clusters. We additionally leverage the model parallel as appropriate to optimize performance. In ablation studies, all models are trained on a sampled corpus from our corpus with 300B tokens. In order to reduce the fluctuation of Losses and PPLs in the tables below, we compute the average Losses and PPLs of the last 1k iterations as the final metrics.

5.1 Architecture Ablations

Transformer *vs* TransNormerLLM   We carried out a meticulous series of comparative tests between our TransNormerLLM and Transformer, spanning over an array of disparate sizes. The comparative performance of these models is clearly illustrated in Table 3. Under identical configurations, it becomes evident that our TransNormerLLM exhibits a superior performance profile compared to Transformer. We observed that TransNormerLLM outperformed Transformer by a remarkable 5% at the size of 385M. More importantly, as the size reached 1B, this superiority became even more pronounced, with an advantage of 9% for TransNormerLLM over Transformer.

Table 3: **Transformer *vs* TransNormerLLM.** TransNormerLLM performs better than Transformer in size of 385M and 1B under identical configurations by 5% and 9%, respectively.

Model Size	385M			1B		
Method	Updates	Loss	PPL	Updates	Loss	PPL
Transformer	100K	2.362	5.16	100K	2.061	4.765
TransNormerLLM	100K	2.247	4.765	100K	1.896	3.728

TransNormer *vs* TransNormerLLM   We compare the original TransNormer and the improved TransNormerLLM and the results are shown in Table 4. TransNormerLLM exhibited an enhancement of 2% and 1% respectively, while significantly faster.

Table 4: **TransNormer *vs* TransNormerLLM.** TransNormerLLM leads the best results.

Method	Params	Updates	Loss	PPL
TransNormerLLM	385M	100K	2.247	4.765
TransNormer-T1	379M	100K	2.290	4.910
TransNormer-T2	379M	100K	2.274	4.858

Positional Encoding   In the positional encoding experiment, we conducted a series of tests, comparing LRPE-d, APE (absolute positional encoding), LRPE, and Exp-Decay (exponential decay). As evident from Table 5, our proposed enhancement has already shown an improvement over the original model. Moreover, the final scheme demonstrated a 2% improvement over the LRPE method.

Table 5: **Positional encoding.** The combination of LRPE+LRPE-d leads the most optimal outcome.

PE Methods	Params	Updates	Loss	PPL
LRPE-d	385M	100K	2.247	4.765
APE	386M	100K	2.387	5.253
LRPE	385M	100K	2.287	4.899
Exp-Decay	385M	100K	2.267	4.834

We also perform ablations on the decay temperature $\left(1 - \frac{l}{L}\right)$ in Eq. 2. The perplexity of the TransNormerLLM is reduced by adding the decay temperature, as shown in Table 6.

Table 6: **Ablations on decay temperature.** The results of decay temperature proved to be superior.

Temperature	Params	Updates	Loss	PPL
w/ temperature	385M	100K	2.247	4.765
w/o temperature	385M	100K	2.258	4.804

Gating mechanism We conduct ablation studies to examine the effect of including the gating mechanism. As observed in Table 7, gate enabled the reduction of the loss value from 2.263 to 2.247.

Table 7: **Ablations on gating mechanism.** The performance with the gate proved to be superior.

Gate	Params	Updates	Loss	PPL
w/ gate	385M	100K	2.247	4.765
w/o gate	379M	100K	2.263	4.820

GLA Activation Functions We conducted experiments on the GLA (Gated Linear Units) structure with respect to the activation function. The outcomes from Table 8 reveal that the impact of the activation function on the final results was not substantial. Hence, taking this into account, we opted for $1 + elu$ in our approach.

Table 8: **Ablations on GLA activation functions.** The results obtained from different activation functions were virtually identical.

GLA Act	Params	Updates	Loss	PPL
1+elu	385M	100K	2.247	4.765
Swish	385M	100K	2.236	4.728
No Act	385M	100K	2.281	4.880

GLU Activation Functions We conduct an experiment by removing the activation function within the Gated Linear Units (GLU) structure. As shown in Table 9, the results reveal that this alteration had a negligible impact on the final outcome. As a result, we decide to adopt the Simple Gated Linear Units (SGLU) structure in our final model configuration.

Table 9: **Ablations on GLU activation functions.** The exclusion of the activation function had no negative impact on the results.

GLU Act	Params	Updates	Loss	PPL
No Act	385M	100K	2.247	4.765
Swish	385M	100K	2.254	4.788

Normalization functions In our study, we conducted a series of ablation tests employing various normalization methods including SRMSNorm, RMSNorm and LayerNorm. The results indicate that there is almost no difference among these methods when applied to TransNormer-LLM. Nevertheless, during the course of our testing, we revisited and re-engineered the SRMSNorm using Triton. As it is shown in Figure 3, empirical evidence supports that our modification offers a significant boost in computational speed when operating with larger dimensions, compared to the PyTorch implementation methods.

Table 10: **Normalization functions.** The deviation in results among the bellowing normalization functions is minimal.

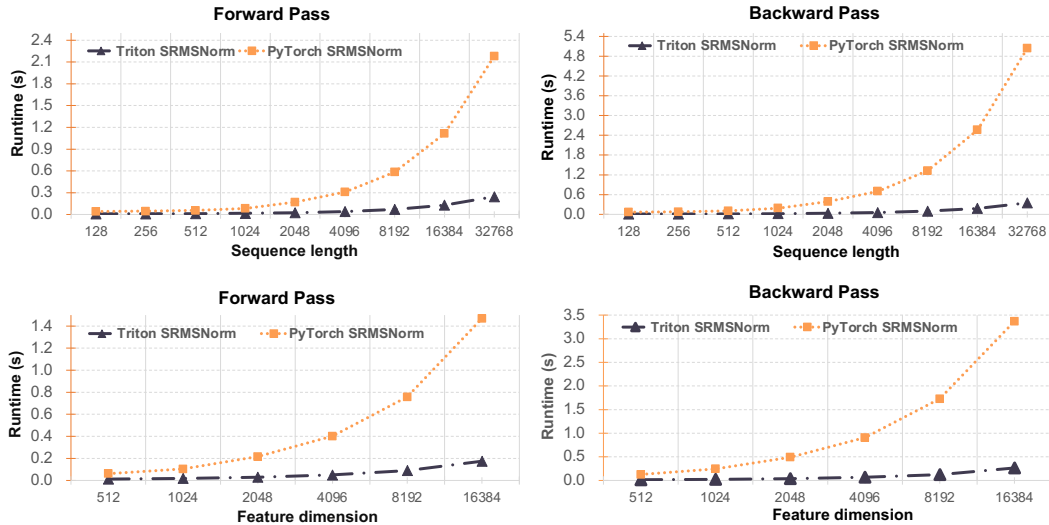| Norm Type	Params	Updates	Loss	PPL
SRMSNorm	385M	100K	2.247	4.765
RMSNorm	385M	100K	2.247	4.766
LayerNorm	385M	100K	2.247	4.765

Figure 3: **Performance Evaluation of SRMSNorm Implementation.** The upper figures exhibit the runtime comparison of the forward pass (left) and backward pass (right) for different sequence lengths, with a fixed feature dimension of 3072. The lower two figures illustrate the runtime comparison for various feature dimensions, with a fixed sequence length of 4096.
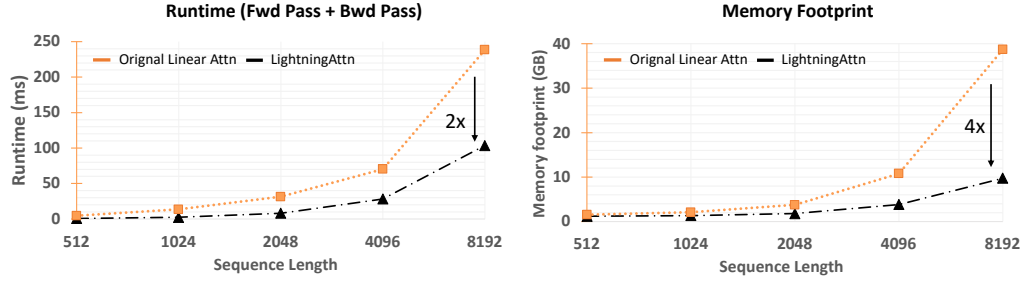
11

Figure 4: **Memory and speed comparison between linear attention and lightning attention.** Left: runtime of forward + backward pass milliseconds for different sequence lengths, with a fixed feature dimension of 2048. Right: memory footprints of forward + backward pass for different sequence lengths, with a fixed feature dimension of 2048.

Lighning Attention We conducted a speed and memory footprint comparison between our Lightning Attention compared and the baseline, which is the PyTorch implementation of the NormAttention [32]. Figure 4 (left) reports the runtime in milliseconds of the forward + backward pass. Runtime grows quadratically with respect to sequence length, but our Lightning Attention operates significantly faster, at least $2\times$ faster than the PyTorch implementation. Figure 4 (right) reports the memory footprint of Lightning Attention compared to the baseline. The memory footprint of Lightning Attention grows linearly with sequence length, which is up to $4\times$ more memory efficient than the baseline when the sequence length is 8192. Our proposed Lightning Attention achieves superior efficiency.
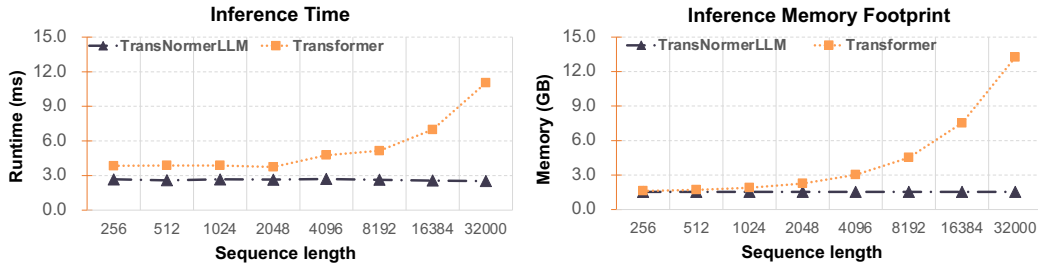

Figure 5: **Inference Time and Memory Footprint.** Left: inference runtime of both forward and backward passes, measured in milliseconds, across different sequence lengths. Right: memory consumption during inference for varying sequence lengths. It is noteworthy that as the sequence length increases, TransNormerLLM demonstrates a consistent inference time and memory footprint.

5.2 System Optimization

5.2.1 Model Parallelism

We conduct a series of experiments with a 7B TransNormerLLM model to investigate the performance of model parallelism on TransNormerLLM in terms of speed and memory. These tests are carried out on a single Nvidia DGX node that houses eight A100 80G GPUs linked by NVLink. In this experiment, FSDP is enabled and Flash Attention [8] is used on the Transformer. Table 11 shows the results for training speed and memory consumption.

It can be seen that model parallelism has a significant effect on memory conservation, as increasing the number of partitions for the model results in lower memory consumption per GPU. Due to NVLink constraints, we kept the dimension of model parallelism within 8 in all of our experiments. The TransNormerLLM-7B model requires only 24.1GB of memory on a single GPU when the model parallel size is set to 8, representing a significant memory reduction of 62.3% when compared to the model parallel size of 1. In comparison, the Transformer-7B model consumes 28.7GB of memory under the same configuration. While model parallelism conserves memory, it is worth noting that training speed is only marginally reduced. TransNormerLLM consistently outperforms Transformer by a wide margin.

Table 11: **Model Parallelism Performance.** We compare the model parallelism performance of Transformer-7B with Flash Attention and TransNormerLLM-7B with Lightning Attention on a single A100 node with NVLink. All experiments use a batch size of 2 and a context length of 2048.

Model	Model Parallel Size	Tokens/s	Allocated Memory/GPU	Memory Saved
Transformer-7B	1	26896.1	66.3 GB	-
	2	24973.7	44.6 GB	32.7%
	4	22375.8	40.2 GB	39.4%
	8	19973.6	28.7 GB	56.7%
TransNormerLLM-7B	1	32048.6	64.0 GB	-
	2	29750.4	41.0 GB	35.9%
	4	27885.2	36.3 GB	43.3%
	8	24280.0	24.1 GB	62.3%

5.2.2 Stress Tests on Model Size and Context Length

A series of stress tests are performed to assess the efficacy of the designed system optimization strategy. The model is scaled up to 175B, which is the largest released version of the TransNormerLLM model. However, this augmentation poses significant training challenges. We use a wide range of distributed training techniques to effectively train such a large model, with the goal of reducing GPU memory consumption while increasing computational and communication efficiencies. To ensure the feasibility of training these massive TransNormerLLM models, Lightning Attention, FSDP, Model Parallelism, AMP, and Activation Checkpointing are used. For the Transformer models, we use Flash Attention [8] in all experiments.

Model Size We perform training experiments on variously sized Transformer and TransNormer-LLM models using a large-scale A100 80G GPU cluster, as shown in Table 12. To achieve the maximum speed for various model sizes, we keep the context length constant at 2048 and increased the batch size until we reached the GPU memory limit. TransNormerLLMs consistently outperform their Transformer counterparts in terms of computation speed. This observation validates the TransNormerLLM model's advantageous linear computational complexity, reinforcing its efficacy.

Table 12: **Efficiency of training models with different sizes.** For comparative purposes, we keep the context length fixed at 2048 and increased the batch size for both transformer and TransNormerLLM to achieve their maximum speeds without encountering out-of-memory issues.

Model	Model Size	Tokens/sec/GPU	Allocated Memory/GPU
Transformer	7B	3362.7	72.5 GB
	13B	1735.6	70.6 GB
	65B	318.2	73.2 GB
	175B	106.2	69.5 GB
TransNormerLLM	7B	4081.0	71.9 GB
	13B	2104.3	73.8 GB
	65B	406.9	69.4 GB
	175B	136.6	70.3 GB

Context Length One of the strengths of TransNormerLLM lies in its utilization of linear attention computation, which exhibits computational and storage complexities linearly correlated with the sequence length. To validate this outstanding characteristic of TransNormerLLM, we conduct training experiments on Transformer and TransNormerLLM models with varying parameter sizes. While maintaining a batch size of 1, we aim to maximize the context length. All experiments run on a small cluster with 64 A100 GPUs. The results, as presented in Table 13, demonstrate the remarkable long context length training capability of TransNormerLLM. Under comparable computational resources, the TransNormerLLM model exhibits the ability to train with longer context lengths compared to conventional Transformer models and achieve higher computational speeds in the process.

Table 13: **Maximum context length for training Transformer and TransNormerLLM.** We compare the maximum context lengths with different model sizes between Transformer and TransNormerLLM on 64 A100 80G GPUs. All experiments use a batch size of 1.

Model	Model Size	Context Length	Relative Speed	Allocated Memory/GPU
Transformer	7B	37K	1	71.1 GB
	13B	24K	1	68.0 GB
	65B	19K	1	73.3 GB
	175B	10K	1	66.9 GB
TransNormerLLM	7B	48K	1.21	65.8 GB
	13B	35K	1.23	61.0 GB
	65B	23K	1.29	68.2 GB
	175B	12K	1.35	63.5 GB

6   Conclusion

We introduced TransNormerLLM in this paper, an improved TransNormer that is tailored for LLMs. Our TransNormerLLM consistently outperformed Transformers in both accuracy and efficiency and can be effectively scaled to 175 billion parameters. Extensive ablations demonstrate the effectiveness of our modifications and innovations in position encoding, gating mechanism, activation functions, normalization functions, and lightning attentions. To support the training of TransNormerLLM, we collected a large corpus that exceeds 6TB and contains over two trillion tokens. A novel self-clean strategy was utilized to ensure data quality and relevance. Our pre-trained models will be released to foster community advancements in efficient LLM.

References

[1] Iz Beltagy, Matthew E. Peters, and Arman Cohan. Longformer: The long-document transformer, 2020.

[2] Stella Biderman, Hailey Schoelkopf, Quentin Anthony, Herbie Bradley, Kyle O'Brien, Eric Hallahan, Mohammad Aflah Khan, Shivanshu Purohit, USVSN Sai Prashanth, Edward Raff, Aviya Skowron, Lintang Sutawika, and Oskar van der Wal. Pythia: A suite for analyzing large language models across training and scaling, 2023.

[3] Tom Brown, Benjamin Mann, Nick Ryder, Melanie Subbiah, Jared D Kaplan, Prafulla Dhariwal, Arvind Neelakantan, Pranav Shyam, Girish Sastry, Amanda Askell, et al. Language models are few-shot learners. *Advances in neural information processing systems*, 33:1877–1901, 2020.

[4] Rewon Child, Scott Gray, Alec Radford, and Ilya Sutskever. Generating long sequences with sparse transformers, 2019.

[5] Krzysztof Marcin Choromanski, Valerii Likhosherstov, David Dohan, Xingyou Song, Andreea Gane, Tamas Sarlos, Peter Hawkins, Jared Quincy Davis, Afroz Mohiuddin, Lukasz Kaiser, David Benjamin Belanger, Lucy J Colwell, and Adrian Weller. Rethinking attention with performers. In *International Conference on Learning Representations*, 2021.

[6] Aakanksha Chowdhery, Sharan Narang, Jacob Devlin, Maarten Bosma, Gaurav Mishra, Adam Roberts, Paul Barham, Hyung Won Chung, Charles Sutton, Sebastian Gehrmann, Parker Schuh, Kensen Shi, Sasha Tsvyashchenko, Joshua Maynez, Abhishek Rao, Parker Barnes, Yi Tay, Noam Shazeer, Vinodkumar Prabhakaran, Emily Reif, Nan Du, Ben Hutchinson, Reiner Pope, James Bradbury, Jacob Austin, Michael Isard, Guy Gur-Ari, Pengcheng Yin, Toju Duke, Anselm Levskaya, Sanjay Ghemawat, Sunipa Dev, Henryk Michalewski, Xavier Garcia, Vedant Misra, Kevin Robinson, Liam Fedus, Denny Zhou, Daphne Ippolito, David Luan, Hyeontaek Lim, Barret Zoph, Alexander Spiridonov, Ryan Sepassi, David Dohan, Shivani Agrawal, Mark Omernick, Andrew M. Dai, Thanumalayan Sankaranarayana Pillai, Marie Pellat, Aitor Lewkowycz, Erica Moreira, Rewon Child, Oleksandr Polozov, Katherine Lee, Zongwei Zhou, Xuezhi Wang, Brennan Saeta, Mark Diaz, Orhan Firat, Michele Catasta, Jason Wei, Kathy Meier-Hellstern, Douglas Eck, Jeff Dean, Slav Petrov, and Noah Fiedel. Palm: Scaling language modeling with pathways, 2022.

[7] Tri Dao. FlashAttention-2: Faster attention with better parallelism and work partitioning. 2023.

[8] Tri Dao, Daniel Y. Fu, Stefano Ermon, Atri Rudra, and Christopher Ré. FlashAttention: Fast and memory-efficient exact attention with IO-awareness. In *Advances in Neural Information Processing Systems*, 2022.

[9] Tri Dao, Daniel Y. Fu, Khaled Kamal Saab, Armin W. Thomas, Atri Rudra, and Christopher Ré. Hungry hungry hippos: Towards language modeling with state space models. *CoRR*, abs/2212.14052, 2022.

[10] Jacob Devlin, Ming-Wei Chang, Kenton Lee, and Kristina Toutanova. BERT: Pre-training of deep bidirectional transformers for language understanding. In *Proceedings of the 2019 Conference of the North American Chapter of the Association for Computational Linguistics: Human Language Technologies, Volume 1 (Long and Short Papers)*, pages 4171–4186, Minneapolis, Minnesota, June 2019. Association for Computational Linguistics.

[11] Zhengxiao Du, Yujie Qian, Xiao Liu, Ming Ding, Jiezhong Qiu, Zhilin Yang, and Jie Tang. Glm: General language model pretraining with autoregressive blank infilling, 2022.

[12] Daniel Y. Fu, Elliot L. Epstein, Eric Nguyen, Armin W. Thomas, Michael Zhang, Tri Dao, Atri Rudra, and Christopher Ré. Simple hardware-efficient long convolutions for sequence modeling. *CoRR*, abs/2302.06646, 2023.

[13] Albert Gu, Tri Dao, Stefano Ermon, Atri Rudra, and Christopher Re. Hippo: Recurrent memory with optimal polynomial projections, 2020.

[14] Albert Gu, Karan Goel, Ankit Gupta, and Christopher Ré. On the parameterization and initialization of diagonal state space models. In *NeurIPS*, 2022.

[15] Albert Gu, Karan Goel, and Christopher Ré. Efficiently modeling long sequences with structured state spaces. In *The Tenth International Conference on Learning Representations, ICLR 2022, Virtual Event, April 25-29, 2022*. OpenReview.net, 2022.

[16] Ankit Gupta, Albert Gu, and Jonathan Berant. Diagonal state spaces are as effective as structured state spaces. In *NeurIPS*, 2022.

[17] Jordan Hoffmann, Sebastian Borgeaud, Arthur Mensch, Elena Buchatskaya, Trevor Cai, Eliza Rutherford, Diego de Las Casas, Lisa Anne Hendricks, Johannes Welbl, Aidan Clark, Tom Hennigan, Eric Noland, Katie Millican, George van den Driessche, Bogdan Damoc, Aurelia Guy, Simon Osindero, Karen Simonyan, Erich Elsen, Jack W. Rae, Oriol Vinyals, and Laurent Sifre. Training compute-optimal large language models, 2022.

[18] Weizhe Hua, Zihang Dai, Hanxiao Liu, and Quoc V Le. Transformer quality in linear time. *arXiv preprint arXiv:2202.10447*, 2022.

[19] Dhiraj Kalamkar, Dheevatsa Mudigere, Naveen Mellempudi, Dipankar Das, Kunal Banerjee, Sasikanth Avancha, Dharma Teja Vooturi, Nataraj Jammalamadaka, Jianyu Huang, Hector Yuen, et al. A study of bfloat16 for deep learning training. *arXiv preprint arXiv:1905.12322*, 2019.

[20] Jared Kaplan, Sam McCandlish, Tom Henighan, Tom B. Brown, Benjamin Chess, Rewon Child, Scott Gray, Alec Radford, Jeffrey Wu, and Dario Amodei. Scaling laws for neural language models, 2020.

[21] Angelos Katharopoulos, Apoorv Vyas, Nikolaos Pappas, and François Fleuret. Transformers are rnns: Fast autoregressive transformers with linear attention. In *International Conference on Machine Learning*, pages 5156–5165. PMLR, 2020.

[22] Guolin Ke, Di He, and Tie-Yan Liu. Rethinking positional encoding in language pre-training. In *International Conference on Learning Representations*, 2021.

[23] Diederik P. Kingma and Jimmy Ba. Adam: A method for stochastic optimization, 2017.

[24] Mike Lewis, Yinhan Liu, Naman Goyal, Marjan Ghazvininejad, Abdelrahman Mohamed, Omer Levy, Ves Stoyanov, and Luke Zettlemoyer. Bart: Denoising sequence-to-sequence pre-training for natural language generation, translation, and comprehension, 2019.

[25] Zexiang Liu, Dong Li, Kaiyue Lu, Zhen Qin, Weixuan Sun, Jiacheng Xu, and Yiran Zhong. Neural architecture search on efficient transformers and beyond. *arXiv preprint arXiv:2207.13955*, 2022.

[26] Paulius Micikevicius, Sharan Narang, Jonah Alben, Gregory Diamos, Erich Elsen, David Garcia, Boris Ginsburg, Michael Houston, Oleksii Kuchaiev, Ganesh Venkatesh, et al. Mixed precision training. *arXiv preprint arXiv:1710.03740*, 2017.

[27] Adam Paszke, Sam Gross, Francisco Massa, Adam Lerer, James Bradbury, Gregory Chanan, Trevor Killeen, Zeming Lin, Natalia Gimelshein, Luca Antiga, Alban Desmaison, Andreas Kopf, Edward Yang, Zachary DeVito, Martin Raison, Alykhan Tejani, Sasank Chilamkurthy, Benoit Steiner, Lu Fang, Junjie Bai, and Soumith Chintala. Pytorch: An imperative style,

high-performance deep learning library. In *Advances in Neural Information Processing Systems 32*, pages 8024–8035. Curran Associates, Inc., 2019.

[28] Guilherme Penedo, Quentin Malartic, Daniel Hesslow, Ruxandra Cojocaru, Alessandro Cappelli, Hamza Alobeidli, Baptiste Pannier, Ebtesam Almazrouei, and Julien Launay. The refinedweb dataset for falcon llm: Outperforming curated corpora with web data, and web data only, 2023.

[29] Bo Peng, Eric Alcaide, Quentin Anthony, Alon Albalak, Samuel Arcadinho, Huanqi Cao, Xin Cheng, Michael Chung, Matteo Grella, Kranthi Kiran GV, Xuzheng He, Haowen Hou, Przemyslaw Kazienko, Jan Kocon, Jiaming Kong, Bartlomiej Koptyra, Hayden Lau, Krishna Sri Ipsit Mantri, Ferdinand Mom, Atsushi Saito, Xiangru Tang, Bolun Wang, Johan S. Wind, Stansilaw Wozniak, Ruichong Zhang, Zhenyuan Zhang, Qihang Zhao, Peng Zhou, Jian Zhu, and Rui-Jie Zhu. Rwkv: Reinventing rnns for the transformer era, 2023.

[30] Ofir Press, Noah Smith, and Mike Lewis. Train short, test long: Attention with linear biases enables input length extrapolation. In *International Conference on Learning Representations*, 2022.

[31] Zhen Qin, Xiaodong Han, Weixuan Sun, Bowen He, Dong Li, Dongxu Li, Yuchao Dai, Lingpeng Kong, and Yiran Zhong. Toeplitz neural network for sequence modeling. In *The Eleventh International Conference on Learning Representations*, 2023.

[32] Zhen Qin, Xiaodong Han, Weixuan Sun, Dongxu Li, Lingpeng Kong, Nick Barnes, and Yiran Zhong. The devil in linear transformer. In *Proceedings of the 2022 Conference on Empirical Methods in Natural Language Processing*, pages 7025–7041, Abu Dhabi, United Arab Emirates, Dec. 2022. Association for Computational Linguistics.

[33] Zhen Qin, Weixuan Sun, Hui Deng, Dongxu Li, Yunshen Wei, Baohong Lv, Junjie Yan, Lingpeng Kong, and Yiran Zhong. cosformer: Rethinking softmax in attention. In *International Conference on Learning Representations*, 2022.

[34] Zhen Qin, Weixuan Sun, Kaiyue Lu, Hui Deng, Dongxu Li, Xiaodong Han, Yuchao Dai, Lingpeng Kong, and Yiran Zhong. Linearized relative positional encoding, 2023.

[35] Zhen Qin, Yiran Zhong, and Hui Deng. Exploring transformer extrapolation, 2023.

[36] Alec Radford, Karthik Narasimhan, Tim Salimans, and Ilya Sutskever. Improving language understanding by generative pre-training. `https://s3-us-west-2.amazonaws.com/openai-assets/research-covers/language-unsupervised/language_understanding_paper.pdf`, 2018.

[37] Alec Radford, Jeffrey Wu, Rewon Child, David Luan, Dario Amodei, Ilya Sutskever, et al. Language models are unsupervised multitask learners. *OpenAI blog*, 1(8):9, 2019.

[38] Jack W. Rae, Sebastian Borgeaud, Trevor Cai, Katie Millican, Jordan Hoffmann, Francis Song, John Aslanides, Sarah Henderson, Roman Ring, Susannah Young, Eliza Rutherford, Tom Hennigan, Jacob Menick, Albin Cassirer, Richard Powell, George van den Driessche, Lisa Anne Hendricks, Maribeth Rauh, Po-Sen Huang, Amelia Glaese, Johannes Welbl, Sumanth Dathathri, Saffron Huang, Jonathan Uesato, John Mellor, Irina Higgins, Antonia Creswell, Nat McAleese, Amy Wu, Erich Elsen, Siddhant Jayakumar, Elena Buchatskaya, David Budden, Esme Sutherland, Karen Simonyan, Michela Paganini, Laurent Sifre, Lena Martens, Xiang Lorraine Li, Adhiguna Kuncoro, Aida Nematzadeh, Elena Gribovskaya, Domenic Donato, Angeliki Lazaridou, Arthur Mensch, Jean-Baptiste Lespiau, Maria Tsimpoukelli, Nikolai Grigorev, Doug Fritz, Thibault Sottiaux, Mantas Pajarskas, Toby Pohlen, Zhitao Gong, Daniel Toyama, Cyprien de Masson d'Autume, Yujia Li, Tayfun Terzi, Vladimir Mikulik, Igor Babuschkin, Aidan Clark, Diego de Las Casas, Aurelia Guy, Chris Jones, James Bradbury, Matthew Johnson, Blake Hechtman, Laura Weidinger, Iason Gabriel, William Isaac, Ed Lockhart, Simon Osindero, Laura Rimell, Chris Dyer, Oriol Vinyals, Kareem Ayoub, Jeff Stanway, Lorrayne Bennett, Demis Hassabis, Koray Kavukcuoglu, and Geoffrey Irving. Scaling language models: Methods, analysis & insights from training gopher, 2022.

[39] Teven Le Scao, Thomas Wang, Daniel Hesslow, Lucile Saulnier, Stas Bekman, M Saiful Bari, Stella Biderman, Hady Elsahar, Niklas Muennighoff, Jason Phang, Ofir Press, Colin Raffel, Victor Sanh, Sheng Shen, Lintang Sutawika, Jaesung Tae, Zheng Xin Yong, Julien Launay, and Iz Beltagy. What language model to train if you have one million gpu hours?, 2022.

[40] Mohammad Shoeybi, Mostofa Patwary, Raul Puri, Patrick LeGresley, Jared Casper, and Bryan Catanzaro. Megatron-lm: Training multi-billion parameter language models using model parallelism. *arXiv preprint arXiv:1909.08053*, 2019.

[41] Ross Taylor, Marcin Kardas, Guillem Cucurull, Thomas Scialom, Anthony Hartshorn, Elvis Saravia, Andrew Poulton, Viktor Kerkez, and Robert Stojnic. Galactica: A large language model for science, 2022.

[42] Philippe Tillet, Hsiang-Tsung Kung, and David D. Cox. Triton: an intermediate language and compiler for tiled neural network computations. *Proceedings of the 3rd ACM SIGPLAN International Workshop on Machine Learning and Programming Languages*, 2019.

[43] Hugo Touvron, Thibaut Lavril, Gautier Izacard, Xavier Martinet, Marie-Anne Lachaux, Timothée Lacroix, Baptiste Rozière, Naman Goyal, Eric Hambro, Faisal Azhar, Aurelien Rodriguez, Armand Joulin, Edouard Grave, and Guillaume Lample. Llama: Open and efficient foundation language models. *arXiv preprint arXiv:2302.13971*, 2023.

[44] Ashish Vaswani, Noam Shazeer, Niki Parmar, Jakob Uszkoreit, Llion Jones, Aidan N Gomez, Łukasz Kaiser, and Illia Polosukhin. Attention is all you need. *Advances in neural information processing systems*, 30, 2017.

[45] BigScience Workshop, :, Teven Le Scao, Angela Fan, Christopher Akiki, Ellie Pavlick, Suzana Ilić, Daniel Hesslow, Roman Castagné, Alexandra Sasha Luccioni, François Yvon, Matthias Gallé, Jonathan Tow, Alexander M. Rush, Stella Biderman, Albert Webson, Pawan Sasanka Ammanamanchi, Thomas Wang, Benoît Sagot, Niklas Muennighoff, Albert Villanova del Moral, Olatunji Ruwase, Rachel Bawden, Stas Bekman, Angelina McMillan-Major, Iz Beltagy, Huu Nguyen, Lucile Saulnier, Samson Tan, Pedro Ortiz Suarez, Victor Sanh, Hugo Laurençon, Yacine Jernite, Julien Launay, Margaret Mitchell, Colin Raffel, Aaron Gokaslan, Adi Simhi, Aitor Soroa, Alham Fikri Aji, Amit Alfassy, Anna Rogers, Ariel Kreisberg Nitzav, Canwen Xu, Chenghao Mou, Chris Emezue, Christopher Klamm, Colin Leong, Daniel van Strien, David Ifeoluwa Adelani, Dragomir Radev, Eduardo González Ponferrada, Efrat Levkovizh, Ethan Kim, Eyal Bar Natan, Francesco De Toni, Gérard Dupont, Germán Kruszewski, Giada Pistilli, Hady Elsahar, Hamza Benyamina, Hieu Tran, Ian Yu, Idris Abdulmumin, Isaac Johnson, Itziar Gonzalez-Dios, Javier de la Rosa, Jenny Chim, Jesse Dodge, Jian Zhu, Jonathan Chang, Jörg Frohberg, Joseph Tobing, Joydeep Bhattacharjee, Khalid Almubarak, Kimbo Chen, Kyle Lo, Leandro Von Werra, Leon Weber, Long Phan, Loubna Ben allal, Ludovic Tanguy, Manan Dey, Manuel Romero Muñoz, Maraim Masoud, María Grandury, Mario Šaško, Max Huang, Maximin Coavoux, Mayank Singh, Mike Tian-Jian Jiang, Minh Chien Vu, Mohammad A. Jauhar, Mustafa Ghaleb, Nishant Subramani, Nora Kassner, Nurulaqilla Khamis, Olivier Nguyen, Omar Espejel, Ona de Gibert, Paulo Villegas, Peter Henderson, Pierre Colombo, Priscilla Amuok, Quentin Lhoest, Rheza Harliman, Rishi Bommasani, Roberto Luis López, Rui Ribeiro, Salomey Osei, Sampo Pyysalo, Sebastian Nagel, Shamik Bose, Shamsuddeen Hassan Muhammad, Shanya Sharma, Shayne Longpre, Somaieh Nikpoor, Stanislav Silberberg, Suhas Pai, Sydney Zink, Tiago Timponi Torrent, Timo Schick, Tristan Thrush, Valentin Danchev, Vassilina Nikoulina, Veronika Laippala, Violette Lepercq, Vrinda Prabhu, Zaid Alyafeai, Zeerak Talat, Arun Raja, Benjamin Heinzerling, Chenglei Si, Davut Emre Taşar, Elizabeth Salesky, Sabrina J. Mielke, Wilson Y. Lee, Abheesht Sharma, Andrea Santilli, Antoine Chaffin, Arnaud Stiegler, Debajyoti Datta, Eliza Szczechla, Gunjan Chhablani, Han Wang, Harshit Pandey, Hendrik Strobelt, Jason Alan Fries, Jos Rozen, Leo Gao, Lintang Sutawika, M Saiful Bari, Maged S. Al-shaibani, Matteo Manica, Nihal Nayak, Ryan Teehan, Samuel Albanie, Sheng Shen, Srulik Ben-David, Stephen H. Bach, Taewoon Kim, Tali Bers, Thibault Fevry, Trishala Neeraj, Urmish Thakker, Vikas Raunak, Xiangru Tang, Zheng-Xin Yong, Zhiqing Sun, Shaked Brody, Yallow Uri, Hadar Tojarieh, Adam Roberts, Hyung Won Chung, Jaesung Tae, Jason Phang, Ofir Press, Conglong Li, Deepak Narayanan, Hatim Bourfoune, Jared Casper, Jeff Rasley, Max Ryabinin, Mayank Mishra, Minjia Zhang, Mohammad Shoeybi, Myriam Peyrounette, Nicolas Patry, Nouamane Tazi, Omar Sanseviero, Patrick von Platen, Pierre Cornette, Pierre François Lavallée, Rémi Lacroix, Samyam Rajbhandari, Sanchit Gandhi, Shaden Smith, Stéphane Requena, Suraj Patil, Tim Dettmers, Ahmed Baruwa, Amanpreet Singh, Anastasia Cheveleva, Anne-Laure Ligozat, Arjun Subramonian, Aurélie Névéol, Charles Lovering, Dan Garrette, Deepak Tunuguntla, Ehud Reiter, Ekaterina Taktasheva, Ekaterina Voloshina, Eli Bogdanov, Genta Indra Winata, Hailey Schoelkopf, Jan-Christoph Kalo, Jekaterina Novikova, Jessica Zosa Forde, Jordan Clive, Jungo Kasai, Ken Kawamura, Liam Hazan, Marine Carpuat, Miruna Clinciu, Najoung Kim, Newton Cheng, Oleg Serikov, Omer Antverg, Oskar van der Wal, Rui Zhang, Ruochen Zhang, Sebastian Gehrmann, Shachar Mirkin, Shani Pais, Tatiana Shavrina, Thomas Scialom, Tian Yun, Tomasz Limisiewicz, Verena Rieser, Vitaly Protasov, Vladislav Mikhailov, Yada Pruksachatkun, Yonatan Belinkov, Zachary Bamberger, Zdeněk Kasner, Alice Rueda, Amanda Pestana, Amir Feizpour, Ammar Khan, Amy Faranak, Ana San-

tos, Anthony Hevia, Antigona Unldreaj, Arash Aghagol, Arezoo Abdollahi, Aycha Tammour, Azadeh HajiHosseini, Bahareh Behroozi, Benjamin Ajibade, Bharat Saxena, Carlos Muñoz Ferrandis, Daniel McDuff, Danish Contractor, David Lansky, Davis David, Douwe Kiela, Duong A. Nguyen, Edward Tan, Emi Baylor, Ezinwanne Ozoani, Fatima Mirza, Frankline Ononiwu, Habib Rezanejad, Hessie Jones, Indrani Bhattacharya, Irene Solaiman, Irina Sedenko, Isar Nejadgholi, Jesse Passmore, Josh Seltzer, Julio Bonis Sanz, Livia Dutra, Mairon Samagaio, Maraim Elbadri, Margot Mieskes, Marissa Gerchick, Martha Akinlolu, Michael McKenna, Mike Qiu, Muhammed Ghauri, Mykola Burynok, Nafis Abrar, Nazneen Rajani, Nour Elkott, Nour Fahmy, Olanrewaju Samuel, Ran An, Rasmus Kromann, Ryan Hao, Samira Alizadeh, Sarmad Shubber, Silas Wang, Sourav Roy, Sylvain Viguier, Thanh Le, Tobi Oyebade, Trieu Le, Yoyo Yang, Zach Nguyen, Abhinav Ramesh Kashyap, Alfredo Palasciano, Alison Callahan, Anima Shukla, Antonio Miranda-Escalada, Ayush Singh, Benjamin Beilharz, Bo Wang, Caio Brito, Chenxi Zhou, Chirag Jain, Chuxin Xu, Clémentine Fourrier, Daniel León Periñán, Daniel Molano, Dian Yu, Enrique Manjavacas, Fabio Barth, Florian Fuhrimann, Gabriel Altay, Giyaseddin Bayrak, Gully Burns, Helena U. Vrabec, Imane Bello, Ishani Dash, Jihyun Kang, John Giorgi, Jonas Golde, Jose David Posada, Karthik Rangasai Sivaraman, Lokesh Bulchandani, Lu Liu, Luisa Shinzato, Madeleine Hahn de Bykhovetz, Maiko Takeuchi, Marc Pàmies, Maria A Castillo, Marianna Nezhurina, Mario Sänger, Matthias Samwald, Michael Cullan, Michael Weinberg, Michiel De Wolf, Mina Mihaljcic, Minna Liu, Moritz Freidank, Myungsun Kang, Natasha Seelam, Nathan Dahlberg, Nicholas Michio Broad, Nikolaus Muellner, Pascale Fung, Patrick Haller, Ramya Chandrasekhar, Renata Eisenberg, Robert Martin, Rodrigo Canalli, Rosaline Su, Ruisi Su, Samuel Cahyawijaya, Samuele Garda, Shlok S Deshmukh, Shubhanshu Mishra, Sid Kiblawi, Simon Ott, Sinee Sang-aroonsiri, Srishti Kumar, Stefan Schweter, Sushil Bharati, Tanmay Laud, Théo Gigant, Tomoya Kainuma, Wojciech Kusa, Yanis Labrak, Yash Shailesh Bajaj, Yash Venkatraman, Yifan Xu, Yingxin Xu, Yu Xu, Zhe Tan, Zhongli Xie, Zifan Ye, Mathilde Bras, Younes Belkada, and Thomas Wolf. Bloom: A 176b-parameter open-access multilingual language model, 2023.

[46] Susan Zhang, Stephen Roller, Naman Goyal, Mikel Artetxe, Moya Chen, Shuohui Chen, Christopher Dewan, Mona Diab, Xian Li, Xi Victoria Lin, Todor Mihaylov, Myle Ott, Sam Shleifer, Kurt Shuster, Daniel Simig, Punit Singh Koura, Anjali Sridhar, Tianlu Wang, and Luke Zettlemoyer. Opt: Open pre-trained transformer language models, 2022.

[47] Yanli Zhao, Andrew Gu, Rohan Varma, Liang Luo, Chien-Chin Huang, Min Xu, Less Wright, Hamid Shojanazeri, Myle Ott, Sam Shleifer, et al. Pytorch fsdp: experiences on scaling fully sharded data parallel. *arXiv preprint arXiv:2304.11277*, 2023.

[48] Lin Zheng, Chong Wang, and Lingpeng Kong. Linear complexity randomized self-attention mechanism. In *International Conference on Machine Learning*, pages 27011–27041. PMLR, 2022.

[49] Lin Zheng, Jianbo Yuan, Chong Wang, and Lingpeng Kong. Efficient attention via control variates. In *International Conference on Learning Representations*, 2023.